Pergamon

Geochimica et Cosmochimica Acta, Vol. 67, No. 14, pp. 2695–2709, 2003

0016-7037/03 $30.00 + .00

doi:10.1016/S0016-7037(03)00107-8

Chromite-Plagioclase assemblages as a new shock indicator; implications for the shock and thermal histories of ordinary chondrites

ALAN E. RUBIN

Institute of Geophysics and Planetary Physics University of California Los Angeles, CA 90095-1567, USA

Abstract—Chromite in ordinary chondrites (OC) can be used as a shock indicator. A survey of 76 equilibrated H, L and LL chondrites shows that unshocked chromite grains occur in equant, subhedral and rounded morphologies surrounded by silicate or intergrown with metallic Fe-Ni and/or troilite. Some unmelted chromite grains are fractured or crushed during whole-rock brecciation. Others are transected by opaque veins; the veins form when impacts cause localized heating of metal-troilite intergrowths above the Fe-FeS eutectic (988°C), mobilization of metal-troilite melts, and penetration of the melt into fractures in chromite grains. Chromite-plagioclase assemblages occur in nearly every shock-stage S3-S6 OC; the assemblages range in size from 20–300 μm and consist of 0.2–20-μm-size euhedral, subhedral, anhedral and rounded chromite grains surrounded by plagioclase or glass of plagioclase composition. Plagioclase has a low impedance to shock compression. Heat from shock-melted plagioclase caused adjacent chromite grains to melt; chromite grains crystallized from this melt. Those chromite grains in the assemblages that are completely surrounded by plagioclase are generally richer in Al_2O_3 than unmelted, matrix chromite grains in the same meteorite. Chromite veinlets (typically 0.5–2 μm thick and 10–300 μm long) occur typically in the vicinity of chromite-plagioclase assemblages. The veinlets formed from chromite-plagioclase melts that were injected into fractures in neighboring silicate grains; chromite crystallized in the fractures and the residual plagioclase-rich melt continued to flow, eventually pooling to form plagioclase-rich melt pockets. Chromite-rich "chondrules" (consisting mainly of olivine, plagioclase-normative mesostasis, and 5–15 vol.% chromite) occur in many shocked OC and OC regolith breccias but they are absent from primitive type-3 OC. They may have formed by impact melting chromite, plagioclase and adjacent mafic silicates during higher-energy shock events. The melt was jetted from the impact site and formed droplets due to surface tension. Crystallization of these droplets may have commenced in flight, prior to landing on the parent-body surface.

Chromite-plagioclase assemblages and chromite veinlets occur in 25 out of 25 shock-stage S1 OC of petrologic type 5 and 6 that I examined. Although these rocks contain unstrained olivine with sharp optical extinction, most possess other shock indicators such as extensive silicate darkening, numerous occurrences of metallic Cu, polycrystalline troilite, and opaque veins. It seems likely that these rocks were shocked to levels at least as high as shock-stage S3 and then annealed by heat generated during the shock event. During annealing, the olivine crystal lattices healed but other shock indicators survived. Published Ar-Ar age data for some S1 OC indicate that many shock and annealing events occurred very early in the history of the parent asteroids. The common occurrence of shocked and annealed OC is consistent with collisions being a major mechanism responsible for metamorphosing OC.

1. INTRODUCTION

It has long been recognized that many ordinary chondrites (OC) have been shocked (e.g., Anders, 1964; Heymann, 1967; Wood, 1967; Taylor and Heymann, 1969). Stöffler et al. (1991) classified OC into six categories representing progressive stages of shock metamorphism: S1 (unshocked), S2 (very weakly shocked), S3 (weakly shocked), S4 (moderately shocked), S5 (strongly shocked), and S6 (very strongly shocked). The equilibration shock pressures for the transitions between these shock stages (as revised by Schmitt et al., 1994 and Schmitt and Stöffler, 1995) are: S1-S2, <4–5 GPa; S2-S3, 5–10 GPa; S3-S4, 10–15 GPa; S4-S5, 25–30 GPa; S5-S6, 45–60 GPa. Of the 161 different OC for which shock-stages were assigned by Stöffler et al. (1991) and Rubin (1994), 80% are shock-stage S3 or higher.

A diverse array of petrographic indicators of shock has been identified in OC. In addition to high-pressure phases (i.e., ringwoodite, majorite, plagioclase with the hollandite structure; e.g., Binns et al., 1969; Smith and Mason, 1970; Coleman, 1977; Liu, 1978), shock indicators include undulose and mosaic extinction in olivine, clinoenstatite lamellae on (100) in orthopyroxene, isotropization and melting of plagioclase (producing maskelynite and plagioclase glass), silicate darkening caused by the dispersion of small blebs of metal and troilite inside silicate grains, martensitic metal grains, polycrystalline troilite, metal and troilite veins, rapidly solidified metal-troilite mixtures, numerically abundant occurrences of metallic Cu, impact-melt-rock clasts, melt pockets, narrow glassy pseudotachylite-like veins, and thick veins of silicate melt (e.g., Hornemann and Müller, 1971; Fodor and Keil, 1976; Smith and Goldstein, 1977; Dodd and Jarosewich, 1979; Scott, 1982; Stöffler et al., 1991; Rubin, 1992, 1994; Bennett and McSween, 1996; Rubin et al., 1997).

Non-silicate oxide phases are also affected by shock metamorphism. The most abundant oxide in OC is chromite ($FeCr_2O_4$). It constitutes 0.6 wt.% of the normative mineralogy of average H- and L-group chondrites (Table 4.1 of Dodd, 1981), but it is essentially absent in OC of petrologic type $\leq\sim$3.5 (Huss et al., 1981). Less abundant oxides in OC include ilmenite ($FeTiO_3$), commonly associated with chromite (Snetsinger and Keil, 1969), and rutile (TiO_2), a rare phase mainly associated with ilmenite and chromite (Buseck and Keil, 1966). Magnetite (Fe_3O_4) in OC is largely restricted to highly oxidized

Table 1. Ordinary chondrites examined in this study.

Acfer 002 H5, S1	Dar al Gani 016 H5, S1	Jartai L6, S4	Queen's Mercy H6, S2
Acfer 100 H6, S1	Dar al Gani 211 H6, S1	Kemouvé H6, S1	Raguli H3.8, S2
Acfer 105 L6, S1	Dar al Gani 324 H6, S1	Kingfisher L5, S5	Red Dry Lake 002 H6, S1
Acfer 118 L6, S1	Dhurmsala LL6, S3	La Criolla L6, S4	Red Dry Lake 005 H6, S1
Acfer 173 H6, S1	Elbert LL6, S2	Lost City H5, S4	Richardton H5, S2
Acfer 314 H6, S1	Elenovka L5, S3	Lunan H6, S3	Rose City H-imb, S6
Alfianello L6, S5	Enshi H5, S4	Magombedze H5, S3	Sixiangou L6, S5
Allegan H5, S1	Ergheo L5, S3	Mayfield H4, S3	Smyer H-imb, S6
Alta'ameem LL5, S2	Estacado H6, S1	MIL 99301 LL6, S1	Spade H-imb, S2
Bald Mountain L4, S4	Farmington L5, S4	Mount Browne H6, S3	Stratford L6, S4
Barwell L6, S3	Farmville H4, S3	NWA 108 L6, S4	Suizhou L6, S4
Bluewing 002 H5, S1	Faucett H4, S4	NWA 141 H5, S2	Superior Valley 005 H6, S1
Bluewing 005 L5, S1	Forest Vale H4, S2	NWA 309 L5, S2	Tuxtuac LL5, S2
Butsura H6, S3	Gilgoin H5, S4	NWA 428 L6, S1	Wuan H6, S3
Charsonville H6, S4	Goodland L4, S4	NWA 792 L5, S1	Xingyang H6, S2
Château-Renard L6, S5	Guareña H6, S1	Ogi H6, S2	Zag H-rb, S2
Chico L-imb, S6	Hedjaz L3.7, S4	Oro Grande H5-fb, S1	Zaoyang H5, S4
Dar al Gani 007 H6, S1	Hualapai Wash L6, S4	Pinto Mountains L6, S5	Zavid L6, S4
Dar al Gani 008 L6, S1	Innisfree L5, S2	Portales Valley H6, S1	Zhovtnevyi H6, S3

imb = impact-melt breccia; rb = regolith breccia; fb = fragmental breccia.
It is possible that some of the specimens from Acfer, Dar al Gani, and Red Dry Lake are paired.

type-3 specimens (Taylor et al., 1981; Krot et al., 1997). Hercynitic spinel [$(Mg,Fe)Al_2O_4$] is confined to rare refractory inclusions in type-3 OC (Noonan and Nelen, 1976; Bischoff and Keil, 1984). In this paper I examine evidence indicating that chromite textures offer a new petrographic indicator of shock.

2. ANALYTICAL PROCEDURES

Thin sections of 76 OC (Table 1) were examined microscopically in transmitted and reflected light. The sizes of chromite-plagioclase assemblages and constituent grains were measured microscopically in reflected light with a calibrated reticle. Mineral compositions were determined with the UCLA JEOL electron microprobe using natural and synthetic standards, 20-s counting times, and ZAF corrections.

3. RESULTS

3.1. Major Petrographic Varieties of Chromite in Ordinary Chondrites

Ramdohr (1967, 1973) identified several varieties of chromite in OC but did not specifically attribute a shock origin to any of them. I have updated and augmented Ramdohr's categories and list six petrographic varieties of chromite (Table 2). As shown below, all of the varieties of chromite were affected by impact processes except the first variety, i.e., coarse blocky chromite grains that lack fractures and opaque veins.

Table 2. Petrographic varieties of chromite in ordinary chondrites.

variety	description
1	Unmelted, unfractured chromite grains
2	Unmelted, impact-fractured chromite grains
3	Chromite grains transected by opaque veins
4	Chromite-plagioclase assemblages
5	Veinlets containing chromite needles and blebs
6	Chromite-rich chondrules

Variety 1. Unmelted, unfractured chromite grains.

In equilibrated OC of low shock stage, chromite occurs as grains surrounded by mafic silicates (with or without adjacent plagioclase) and as grains intergrown with metallic Fe-Ni and/or troilite (e.g., Fig. 1a; Figs. C1, C8 of Ramdohr, 1973). The chromite grains range from ~10–200-μm in size (typically 50–100 μm) and occur in blocky, equant, subhedral, anhedral, and rounded morphologies. These unshocked chromite grains were called "coarse chromite" by Ramdohr (1967, 1973). With increasing petrologic type, chromite tends to become richer in FeO, MnO and Al_2O_3 (Bunch et al., 1967).

Variety 2. Unmelted, fractured chromite grains.

In some weakly to moderately shocked OC, unmelted chromite grains have been fractured or crushed by impact processes. Jartai contains chromite grains with several irregular fractures (Fig. 1b). Mt. Browne contains partly crushed chromite grains with numerous fractures; similar fractures occur in adjacent silicates.

Variety 3. Chromite grains transected by opaque veins.

In some shocked OC, unmelted chromite grains are incised or transected by 1–10-μm-thick veins of troilite or metallic Fe-Ni (e.g., Fig. 2b of Rubin et al., 2002). Some of the transected chromite grains are intergrown with coarse grains of metallic Fe-Ni and troilite; others are completely surrounded by mafic silicate that has itself been invaded by opaque veins (Fig. 1c,d). The modal abundance of opaque veins in the transected chromite grains varies from ~1–25 vol.%. An unmelted, but severely fractured chromite grain containing small veinlets of metallic Fe-Ni and sulfide was reported by Kring et al. (1996) in a shocked L5 clast in the Cat Mountain OC impact-melt breccia.

Variety 4. Chromite-plagioclase assemblages.

In shocked equilibrated OC, some chromite occurs in chromite-plagioclase assemblages (e.g., Fig. 2; Figs. C9, C12 of

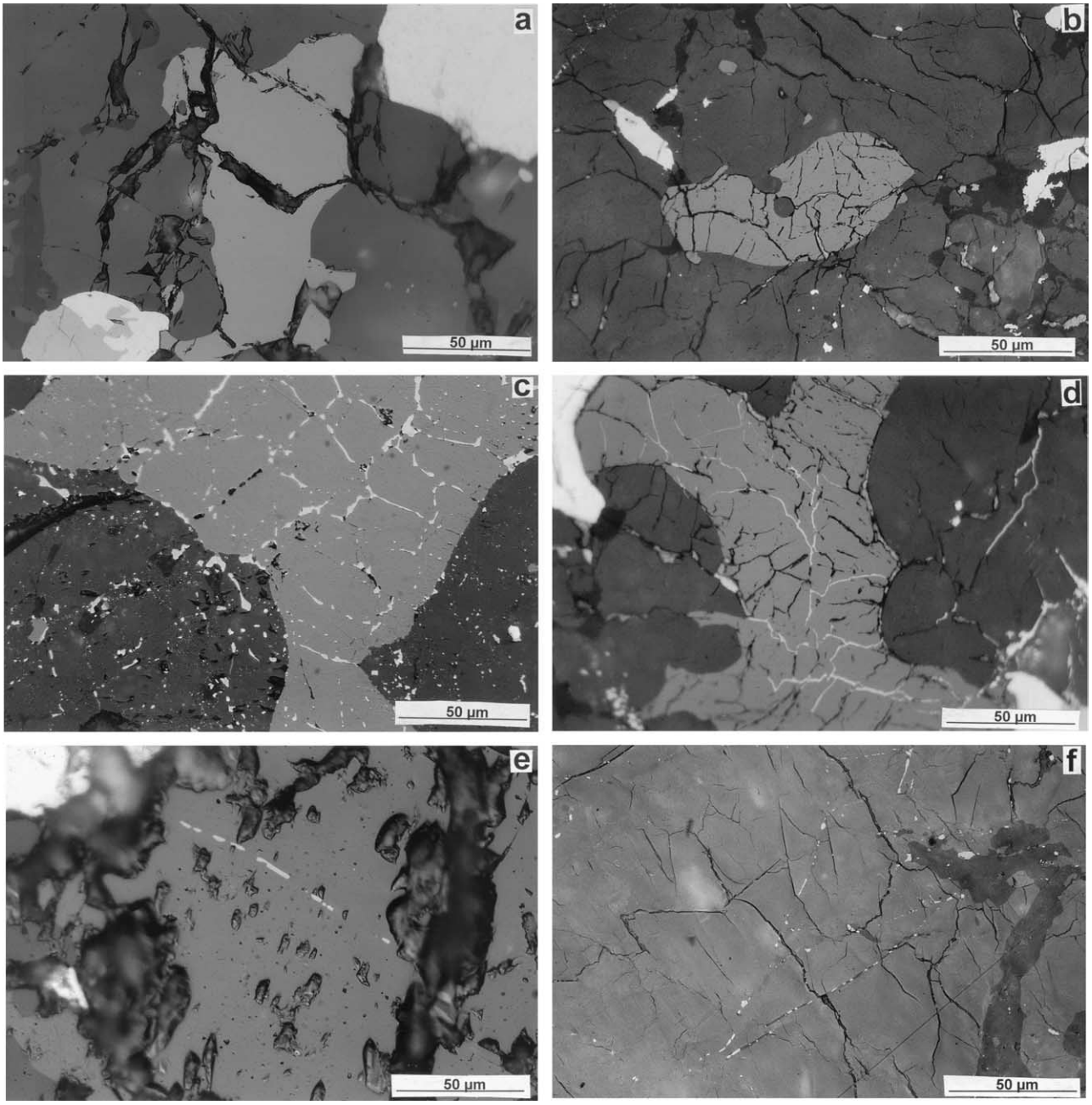

Fig. 1. Petrographic varieties of chromite in ordinary chondrites. (a) Unmelted chromite grain (medium gray) in Kernouvé (H6, S1) surrounded by silicate (dark gray) and adjacent to metallic Fe-Ni (white) and troilite (light gray). Black areas are plucked regions formed during thin-section preparation. (b) Unmelted, but fractured chromite grain (medium gray) in Jartai (L6, S4). Similar fractures (narrow black lines) occur in the surrounding silicate grains. (c) Unmelted chromite grain (medium gray) transected by numerous thin troilite veins (white) in Rose City (H-chondrite impact-melt breccia, S6). The troilite veins also occur in the surrounding silicate grains. (d) Unmelted chromite grain (medium gray) containing very thin veins of troilite (white) in Jartai (L6, S4). A few troilite veins also occur in the surrounding silicate. (e) Chromite needles (light gray) forming a veinlet transecting silicate grains (dark gray) in Portales Valley (H6, S1). (f) Chromite veinlets (light gray), some with interstitial glass of plagioclase composition (dark gray), within silicate grains (medium gray) in Jartai (L6, S4). At right is a melt pocket (dark gray) consisting of plagioclase glass. All images in reflected light and to the same scale.

Ramdohr, 1973). These assemblages were referred to as "clusters of chromite aggregates" by Ramdohr (1967, 1973) and have been reported in many OC including H4 Broken Bow, H6 Cavour, L5 Farmington, H5 Forest City, L6 Kyushu, L6 Narellen, H5 Nardoo (no. 1), the Zag H-chondrite regolith breccia, and the Ramsdorf and Smyer impact-melt breccias (Begemann and Wlotzka, 1969; Ramdohr, 1973; Ashworth, 1985; Rubin, 2002a; Rubin et al., 2002). L6 Paranaiba (S6) contains chromite droplets dispersed within maskelynite (Keil et al., 1977). A related inclusion in L6 Los Martinez consists of crystalline

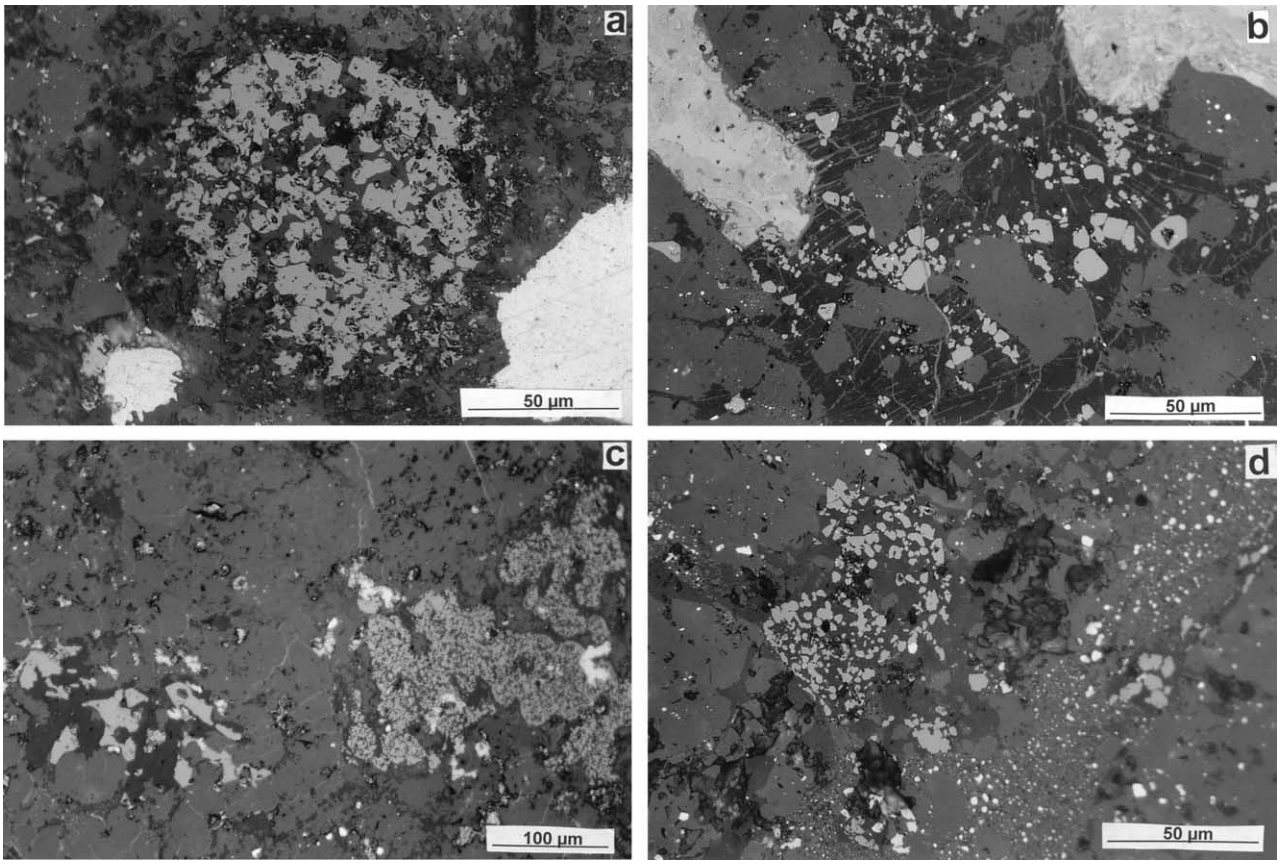

Fig. 2. Chromite-plagioclase assemblages in ordinary chondrites. (a) Round assemblage A containing much more chromite than plagioclase in the Rose City impact-melt breccia. (b) Network A of interconnected assemblages containing much more plagioclase than chromite in the Chico impact-melt breccia. Large light-gray masses at upper left and upper right are limonite patches formed from terrestrially weathered metallic Fe-Ni grains. Gray lines transecting the plagioclase are veins of limonite. (c) Fine-grained chromite-plagioclase assemblage A (right) and coarse-grained assemblage A' (left) in Hualapai Wash. The assemblages have very different plagioclase/chromite modal abundance ratios, i.e., 0.3 and 2, respectively. The coarse chromite grains in assemblage A' may be unmelted grain fragments. (d) Medium-grained chromite-plagioclase assemblage (assemblage B; left of center) near a thick silicate-rich shock vein (right of center) containing numerous small blebs of metallic Fe-Ni in Farmington. All images in reflected light.

plagioclase intergrown with chromium-rich spinel (Brearley et al., 1991).

The assemblages vary widely in size, texture, grain size and the proportions of chromite and plagioclase. They range from 20–300 μm in size and consist of 0.2–20-μm-size euhedral, subhedral, anhedral and rounded chromite grains surrounded by plagioclase. Chromite grains constitute 10–75 vol.% of these assemblages. They are described in more detail below.

Variety 5. Chromite veinlets.

Curvilinear trails or veinlets of chromite needles and small rounded chromite blebs occur in many shocked OC where they transect mafic silicate grains (e.g., Fig. 4d of Rubin, 1992). The veinlets are typically 0.5–2-μm thick and range in length from ~10 to 300 μm. Many chromite veinlets occur in the vicinity (typically within a few hundred micrometers) of chromite-plagioclase assemblages. The vast majority of veinlets consist exclusively of chromite (Fig. 1e); a few veinlets also contain plagioclase or glass of plagioclase composition (Fig. 1f).

Variety 6. Chromite-rich chondrules.

In shocked, equilibrated OC and in OC regolith breccias, there are rare chondrules that consist of 85–95 vol.% silicate (mainly olivine and plagioclase-normative mesostasis) and 5–15 vol.% chromite (e.g., Figs. 4, 9 of Ramdohr, 1967). These objects have cryptocrystalline, radial, barred and porphyritic textures (Fig. 3; they were described by Ramdohr (1967) as chromite chondrules and Krot and Rubin (1993) as chromite-bearing silicate chondrules.

A. N. Krot and A. E. Rubin (unpublished data) found 50 chromite-rich chondrules in 43 H, L and LL chondrites and 17 chromite-rich chondrules in 10 solar-gas-rich OC regolith breccias. They estimated that these chondrules constitute ~0.03 vol.% of typical OC whole rocks, ~0.06 vol.% of OC regolith breccias, and ~0.04% of all OC chondrules. However, Krot and Rubin found no chromite-rich chondrules in the 37 type $\leq$3.7 OC that they examined (76.3 cm^2 surface area). The least equilibrated OC in which these chondrules were observed is H3.8 Raguli.

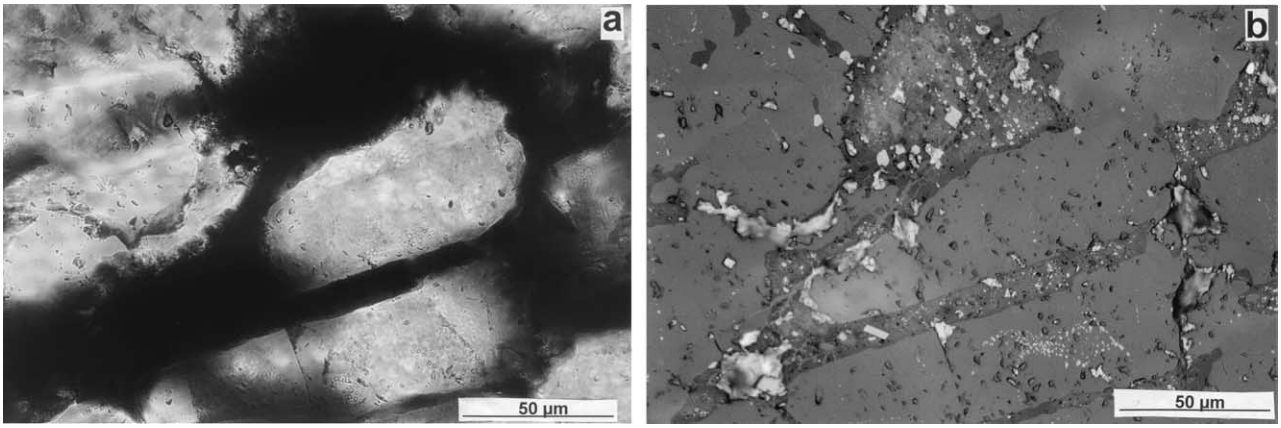

Fig. 3. Chromite-rich barred-olivine Chondrule D in Estacado. (a) Portion of the chondrule showing olivine bars (light gray) and surrounding mesostasis (black). Transmitted light. (b) Same region as (a) showing abundant small chromite grains in the mesostasis. Olivine bar at bottom contains a patch of small chromite blebs. Reflected light. Both images are to the same scale.

3.2. Chromite in shocked ordinary chondrites

Most occurrences of chromite grains transected by opaque veins, chromite-plagioclase assemblages, chromite veinlets, and chromite-rich chondrules occur in shocked meteorites. (Exceptions are discussed below.) Many of the same shocked meteorites also contain blocky, fractured but unmelted chromite grains.

3.2.1. Impact-melt breccias–shock stage S6.

Smyer is an H-chondrite impact-melt breccia that contains ~20 vol.% 0.5- to 13-mm-thick silicate-rich melt veins surrounding unmelted subrounded chondritic clasts that range up to 7 cm (Rubin, 2002a). These chondritic clasts contain a few 100- to 300-μm-size chromite-plagioclase assemblages that consist of 40 to 60 vol.% euhedral to rounded 0.2- to 4-μm-size chromite grains (many intergrown with each other) embedded in plagioclase glass (e.g., Fig. 3 of Rubin, 2002a).

Rose City is an H-chondrite impact-melt breccia containing 60±10 wt.% unmelted chondritic clasts 0.5- to 10-cm in size and 40±10 wt.% impact-melted silicate and metal-troilite (Mason and Wiik, 1966; Bogard, 1979; Rubin, 1995a). Other evidence of shock includes the presence of martensite and absence of kamacite (Rubin, 1990) and extensive silicate darkening caused by the dispersion within mafic silicate grains of complex curvilinear trails of small blebs of metallic Fe-Ni and troilite (Rubin, 1992).

Rose City also contains unmelted chromite grains transected by troilite veins (Fig. 1c), chromite-plagioclase assemblages (Fig. 2a), chromite veinlets and chromite-rich chondrules. The veins constitute ~2–10 vol.% of the chromite grains and range in thickness from 0.5 - 2 μm. Troilite veins transecting neighboring silicate grains are also 0.5 - 2 μm thick (Fig. 1c,d). All of the chromite grains containing troilite veins have 5–30-μm-size troilite grains situated at the chromite-silicate boundary. Most chromite-plagioclase assemblages in Rose City are relatively coarse-grained; the average chromite grain size is 10 μm. Chromite-rich chondrules are typically 300–500 μm in diameter.

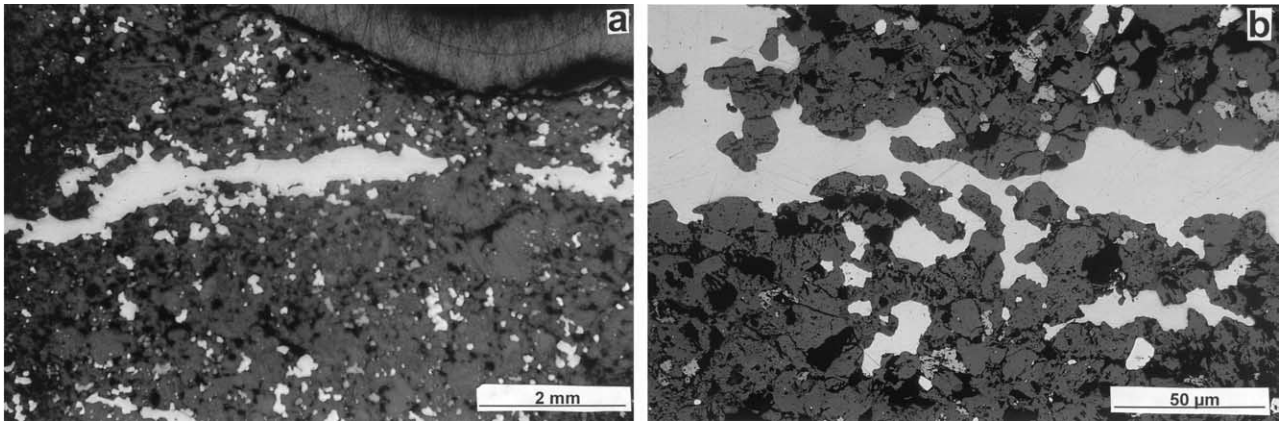

Fig. 4. Metallic Fe-Ni shock vein in Kernouvé. (a) Vein (white) transects silicate grains (dark gray). (b) Portion of vein showing that silicate peninsulas within the vein are preferentially oriented toward the left. This probably resulted from flow of the metallic liquid from right to left. The existence of this shock vein demonstrates that Kernouvé was appreciably shocked before it was annealed to S1 levels. Both images are in reflected light.

Chico is an L-chondrite impact-melt breccia consisting of ~60 vol.% melt and ~40 vol.% relict L6 chondritic material containing disrupted chondrules, numerous shock veins and melt pockets (Bogard et al., 1995). The meteorite also contains chromite-plagioclase assemblages (Fig. 2b) and chromite veinlets. The assemblages average 200 - 300 μm and contain relatively small (2–10-μm-size) chromite grains.

3.2.2. Shock-stage S3-S5 ordinary chondrites.

During this study I observed chromite-plagioclase assemblages and chromite veinlets in nearly every shocked ordinary chondrite that I examined. In addition to occurring in the S6 impact-melt breccias described above, chromite-plagioclase assemblages were identified in some shock-stage S5 OC (L6 Alfianello, L6 Château-Renard, L5 Kingfisher, L6 Pinto Mountains and L6 Sixiangkou), many S4 OC(L4 Bald Mountain, H6 Charsonville, H5 Enshi, L5 Farmington, H4 Faucett, H5 Gilgoin, L4 Goodland, L3.7 Hedjaz, L6 Hualapai Wash, L6 Jartai, L6 La Criolla, H5 Lost City, L6 NWA 108, L6 Stratford, L6 Suizhou and H5 Zaoyang), and some S3 OC (L6 Barwell, H6 Butsura, LL6 Dhurmsala, H4 Farmville, H6 Lunan, H4 Mayfield, H5 Magombedze, H6 Mt. Browne, H6 Wuan and H6 Zhovtnevyi). Selected occurrences in three of these meteorites are described below.

3.2.2.1. Jartai.

Regions containing abundant chromite-plagioclase assemblages and chromite veinlets constitute ~3 vol.% of Jartai (L6, S4). Typical assemblages have small (0.5 - 2 μm) chromite grains, although a few assemblages are somewhat coarser (3–10-μm-size chromite grains). The assemblages range from 10–100 μm in size and are interconnected through networks of plagioclase veins. Abundant chromite veinlets within mafic silicate grains occur among the chromite-plagioclase assemblages. Some chromite veinlets (e.g., Fig. 1f) consist of ~40 vol.% chromite needles and ~60 vol.% plagioclase (or plagioclase glass) separating the chromite needles. The veinlets average 0.8 μm in thickness and range from 50 to 100 μm in length.

3.2.2.2. Hualapai Wash.

Hualapai Wash (L6, S4) contains ~1 vol.% chromite-plagioclase assemblages ranging in size from 70 to 300 μm. Most assemblages are fine-grained (e.g., Fig. 2c), with an average chromite grain size of 2 - 6 μm. However, assemblage A' (Fig. 2c) is much coarser; it consists of ~60 vol.% coarse chromite grains (typically 10 - 60 μm) and ~40 vol.% mesostasis. The coarse chromite grains in this assemblage are angular and appear to be relict, unmelted grain fragments.

3.2.2.3. Farmington.

Approximately 0.2 vol.% of Farmington (L5, S4) consists of regions containing chromite-plagioclase assemblages and associated chromite veinlets. There are two basic varieties of assemblages: those with very-fine-grained chromite (averaging 0.2–0.5 μm) and those of intermediate grain size (averaging ~5 μm) (Fig. 2d). Chromite veinlets are typically 0.5 μm thick and 30–70 μm long. Many of the chromite grains in Farmington are transected by troilite veins. The veins range in thickness from 0.5 to 2 μm; some veins are linear, others are curved and appear to have been sheared. Some troilite veins are connected to 5–12-μm-size troilite grains at the chromite-silicate boundary.

3.2.3. Chromite in shock-stage S1 equilibrated ordinary chondrites.

I observed chromite-plagioclase assemblages and chromite veinlets in 18 out of 18 type-6 shock-stage S1 OC and 7 out of 7 type-5 S1 OC. These meteorites are considered "unshocked" on the basis of the sharp optical extinction in their olivine (Stöffler et al., 1991). Several of these rocks (e.g., Guareña, Estacado, Kernouvé) have been assumed by workers investigating ^{244}Pu fission-track thermometry (e.g., Pellas and Storzer, 1981; Pellas and Fiéni, 1988; Pellas et al., 1990) to have never been shocked. However, these meteorites exhibit other petrographic features consistent with shock metamorphism (e.g., silicate darkening, coarse polycrystalline troilite, metallic Fe-Ni veins). As discussed below, these rocks appear to have been shocked and later annealed.

3.2.3.1. Portales Valley (H6).

Kring et al. (1999) and Rubin et al. (2001) described Portales Valley as an annealed H-chondrite impact-melt breccia containing coarse metal with a Widmanstätten structure interstitial to angular and subrounded chondritic clasts. Most coarse olivine grains exhibit sharp optical extinction, although a few olivine grains exhibit undulose extinction; rare grains contain planar fractures. Chromite-plagioclase assemblages in Portales Valley were noted by D. A. Kring (pers. commun., 1999). One 450×600 μm assemblage described by Rubin et al. (2001) consists of ~80 vol.% plagioclase, ~20 vol.% chromite, 0.4 vol.% troilite, and 0.2 vol.% metallic Fe-Ni. The chromite occurs as small (0.5–4-μm) subangular grains arranged in linear arrays, and 10–60-μm-size rounded and angular grains.

3.2.3.2. Miller Range 99301 (LL6).

Rubin (2002b) interpreted MIL 99301 as a chondrite that experienced successive episodes of thermal metamorphism, shock metamorphism and annealing. All of the olivine and plagioclase exhibit sharp optical extinction characteristic of shock stage S1. In addition to unshocked blocky chromite grains adjacent to silicate, metallic Fe-Ni, and/or troilite, MIL 99301 contains numerous 25–300-μm-size chromite-plagioclase assemblages containing 0.2–10-μm-size euhedral, subhedral, anhedral and rounded chromite grains. Also present in MIL 99301 are networks of intersecting 5–300-μm-long chromite veinlets composed of 1-μm-size chromite blebs and/or 0.5-μm-thick chromite needles.

3.2.3.3. Kernouvé (H6).

Although Kernouvé contains olivine with sharp optical extinction characteristic of shock stage S1 (Rubin, 1992, 1994), elongated metal masses in the rock were recognized as partially obliterated shock veins (Hutson, 1989; Rubin, 1992). Turner et

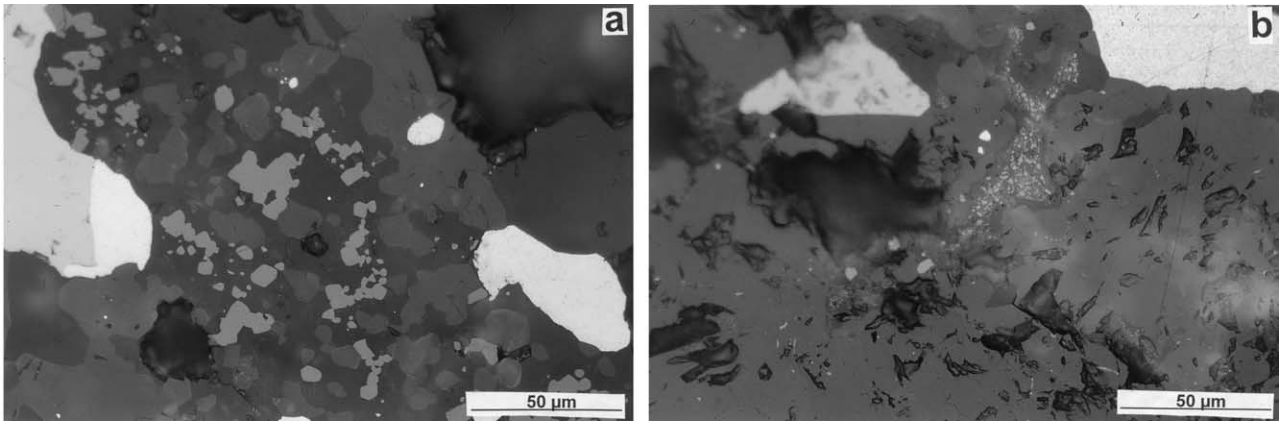

Fig. 5. Chromite-plagioclase assemblages in shock-stage S1, type-6 ordinary chondrites. (a) Small assemblage A' in Kernouvé surrounded by silicate (dark gray) and located near metallic Fe-Ni (white) and troilite (light gray). (b) Small, fine-grained assemblage A in Estacado located near metallic Fe-Ni grains (white). Both images are in reflected light and to the same scale.

al. (1978) reported metal veins in Kernouvé. I report here (Fig. 4a,b) a ~2-cm long, 0.4–1.0-mm-wide metal vein in UCLA specimen LC884 (also present in thin sections LC-1492 and −1493). The Kernouvé metal vein closely resembles metal veins in shocked ordinary chondrites (e.g., Dodd et al., 1982; Rubin, 1985). Kernouvé also contains chromite veinlets (Rubin, 1992) and rare chromite-plagioclase assemblages (Fig. 5a). These assemblages are typically 100×300 μm in size; some are fine grained (0.5–2 μm), others have somewhat coarser grains (5–25 μm).

3.3.3.4. Estacado (H6).

Grady (2000) listed Estacado as shock stage S1, consistent with the sharp optical extinction exhibited by its olivine grains. I report here the presence of a metal vein in UCLA specimen LC153 that is ~6 cm long and 0.5 mm wide. Smaller metal veins also occur. Approximately 0.5 vol.% of Estacado consists of chromite veinlets and associated chromite-plagioclase assemblages (Fig. 5b). Most veinlets are composed of small (0.3–0.5 μm) rounded chromite blebs and/or 0.5×2-μm-size chromite needles; one veinlet consists of small chromite needles and a continuous elongated, curvilinear chromite rod 0.5 ×130 μm in size that fills a fracture. Some chromite veinlets are linear, others are curved; they range from 30 to 100 μm in length. Chromite-plagioclase assemblages are typically 50 μm in size; most contain fine-grained (1–2-μm-size) chromite (Fig. 5b); a few contain somewhat coarser (3–8 μm) chromite grains.

3.2.3.5. Guareña (H6).

Olivine in Guareña exhibits sharp optical extinction, consistent with the meteorite's shock-stage-S1 classification (Grady, 2000). Shock effects in Guareña include moderate silicate darkening (due to the dispersion of small metallic Fe-Ni and troilite grains in silicate interiors), coarse polycrystalline troilite, abundant plessite (Willis and Goldstein, 1983) and several occurrences of metallic Cu. Guareña contains a few 250-μm-size chromite-plagioclase assemblages containing relatively coarse (20–50 μm) grains of chromite.

3.2.3.6. Other type-6 OC.

I examined 13 other petrologic type-6 OC of shock stage S1: H6 Acfer 100, L6 Acfer 105, L6 Acfer 118, H6 Acfer 173, H6 Acfer 314, H6 Dar al Gani 007, L6 Dar al Gani 008, H6 Dar al Gani 211, H6 Dar al Gani 324, L6 NWA 428, H6 Red Dry Lake 002, H6 Red Dry Lake 005, and H6 Superior Valley 005. Each contains chromite-plagioclase assemblages and chromite veinlets; several exhibit silicate darkening and contain metallic Cu and irregular grains of troilite within metallic Fe-Ni. NWA 428 also contains opaque shock veins, metallic Cu, polycrystalline troilite and low-Ca clinopyroxene.

3.2.3.7. Type-5 OC.

Shock features in S1 OC are not limited to those rocks of petrologic type 6. I examined seven petrologic type-5 OC of shock-stage 1: H5 Acfer 002, H5 Allegan, H5 Bluewing 002, L5 Bluewing 005, H5 Dar al Gani 016, L5 NWA 792, and H5 Oro Grande. Each of them contains chromite-plagioclase assemblages and chromite veinlets; Dar al Gani 016 exhibits significant silicate darkening. Other shock features in Allegan include significant silicate darkening (Rubin, 1994) and occurrences of metallic Cu (Ramdohr, 1973). Bluewing 002 contains rapidly solidified metal-troilite intergrowths and melt pockets; Acfer 002, NWA 792 and Bluewing 005 contain metallic Cu and irregular troilite grains within metallic Fe-Ni; the latter two also exhibit silicate darkening. Oro Grande exhibits extensive silicate darkening and contains melt pockets and irregular grains of troilite inside metallic Fe-Ni.

3.2.4. Shock-stage S2 ordinary chondrites.

Chromite-plagioclase assemblages and chromite veinlets occur in some very weakly shocked (i.e., shock-stage S2) OC including LL5 Alta'ameem, LL6 Elbert, L5 Innisfree, H5 NWA 141, L5 NWA 309, H6 Ogi, H6 Queen's Mercy, H5

Table 3. Typical compositions of chromite varieties (wt. %) in ordinary chondrites.

crm var	1	1	2	3	4	4	4	4	4	4	4
meteorite	H W	MIL	Jartai	Farm	MIL	H W	H W	H W	Estacado	Guareña	Jartai
	L6 S4	LL6 S1	L6 S4	L5 S4	LL6 S1	L6 S4	L6 S4	L6 S4	H6 S1	H6 S1	L6 S4
grn/asmb	C'	3	F	F	1	C	A	A'	B	A	E
# grains	2	8	2	3	9	3	3	4	1	4	5
gm prop					gls	frg	srf	frg	gls	gls	gls
SiO_2	<0.04	<0.04	<0.04	<0.04	0.14	0.08	0.51	0.12	0.16	<0.04	0.10
TiO_2	2.0	3.1	2.6	3.1	1.9	2.1	2.1	2.2	1.9	2.4	2.3
Al_2O_3	5.8	5.7	6.4	6.0	11.6	5.7	8.0	5.5	7.1	6.5	6.3
Cr_2O_3	57.6	55.4	57.6	55.8	51.5	57.3	54.0	56.7	55.1	56.7	55.9
FeO	30.6	31.7	28.2	28.0	29.0	31.0	29.7	31.2	28.9	28.9	28.2
MnO	0.58	0.54	0.51	0.46	0.48	0.58	0.57	0.53	0.73	0.64	0.52
MgO	2.4	1.7	4.4	5.6	3.9	2.5	3.0	2.3	3.3	3.6	4.5
CaO	<0.04	<0.04	<0.04	<0.04	0.13	0.08	0.12	<0.04	0.09	<0.04	0.07
total	99.0	98.1	99.7	99.0	98.6	99.3	98.0	98.6	97.3	98.7	97.9

crm var	4	4	4	4	4	4	4	5	6	6	6
meteorite	Farm	Farm	Farm	Farm	Farm	Farm	Kernouvé	Jartai	Estacado	Elenovka[§]	Mag[§]
	L5 S4	L5 S4	L5 S4	L5 S4	L5 S4	L5 S4	H6 S1	L6 S4	H6 S1	L5 S3	H5 S3
grn/asmb	A	A	B	C	C	E	A′	A	D	El1	Mg1a
# grains	1	2	3	2	1	1	3	1	1	10	5
gm prop	gls	srf	gls	gls	srf	gls	gls	srf			
SiO_2	0.10	0.07	0.12	0.14	0.10	0.38	0.06	0.19	0.38	n.a.	n.a.
TiO_2	2.6	5.3*	2.3	2.8	2.7	1.1	2.2	2.8	1.8	2.3	1.2
Al_2O_3	6.7	5.6	7.2	6.7	5.4	10.6	6.5	5.8	7.0	10.6	21.8
Cr_2O_3	57.9	54.0	55.8	56.4	55.6	53.5	56.0	54.9	54.3	55.4	45.1
FeO	26.5	29.2	25.7	26.3	28.1	24.4	29.3	28.6	31.0	26.3	23.7
MnO	0.47	0.48	0.43	0.47	0.55	0.40	0.67	0.46	0.65	0.35	0.59
MgO	5.6	5.0	5.9	6.2	4.6	7.1	3.2	4.5	2.4	4.0	7.9
CaO	<0.04	<0.04	0.17	0.06	0.06	0.19	<0.04	0.16	0.04	n.a.	0.08
total	99.9	99.6	97.6	99.1	97.1	97.7	97.9	97.4	97.6	99.0	100.5

meteorites: H W = Hualapai Wash; MIL = MIL 99301; Farm = Farmington; Mag = Magombedze
crm var = chromite variety; petrographic varieties of chromite listed in Table 2.
grn/asmb = grain or assemblage label; n.a. = not analyzed
grn prop = grain properties: gls—the chromite grain is completely surrounded by plagioclase glass; srf—the chromite grain is at the surface of the assemblage, adjacent to silicate grains in the matrix; frg—the chromite grain appears to be an unmelted grain fragment.
* One grain contains 7.0 wt.% TiO_2.
§ Chromite analyzed by A.N. Krot (unpublished data, 1993). Total in Magombedze Mg1a also includes 0.17 wt.% ZnO.

Richardton, LL5 Tuxtuac, and H6 Xingyang. The assemblages range in size from ~20 - 380 μm; most are fine-grained (1–10 μm), but a few have relatively coarse (~5–100 μm) chromite grains. Most of the veinlets are 25–85 μm long and consist of 0.5×2-μm-size chromite needles; rare veinlets consist of 0.2-μm-size rounded blebs of chromite. The chromite-plagioclase assemblages and chromite veinlets closely resemble those in OC of higher shock stage.

3.2.5. Petrographic associations of chromite and plagioclase.

In shocked OC, most chromite grains adjacent to plagioclase are either in chromite-plagioclase assemblages or are isolated grains that appear to be at least partly melted. These partly melted chromite grains are flanked by small patches of chromite-plagioclase assemblages. However, most chromite and plagioclase grains in equilibrated OC are not adjacent to one another. In the most primitive OC (LL3.0 Semarkona), X-ray maps show no correlations between Al and Cr or between Na and Cr (J. N. Grossman, pers. commun., 2003).

3.3. Mineral chemistry

Compositions of examples of the six petrographic varieties of chromite are listed in Table 3. Different unmelted chromite grains (varieties 1–3) in an individual OC are relatively uniform in composition, consistent with the observations of Snetsinger et al. (1967). The unmelted chromite grains in this study are very similar in composition to those reported previously (Bunch et al., 1967). Bunch et al. found that the composition of chromite grains in equilibrated OC vary systematically with chondrite group: e.g., those in H chondrites contain higher concentrations of Cr_2O_3, MgO and MnO and lower concentrations of FeO than those in L or LL chondrites. These intergroup compositional variations reflect equilibration with mafic sili-

cates (which also increase in FeO content from H to L to LL; e.g., Rubin, 1990; Gomes and Keil, 1980). The limited data on unmelted chromite grains in this study (varieties 1–3; Table 3) are consistent with the intergroup compositional trends identified by Bunch et al. (1967).

Chromite grains within chromite-plagioclase assemblages tend to vary in their concentrations of FeO, MgO, TiO_2 and Al_2O_3. The mean FeO and MgO contents of chromite in the assemblages varies from ~24–31 and ~2–7 wt.%, respectively (Table 3). Rare chromite grains in the chromite-plagioclase assemblages in several shocked chondrites are relatively rich in TiO_2; e.g., one chromite grain within chromite-plagioclase assemblage A in Farmington contains 7.0 wt.% TiO_2 (Table 3). In contrast, Farmington assemblage E chromite contains only 1.1 wt.% TiO_2. Chromite grains near the surface of chromite-plagioclase assemblages (i.e., chromite grains in contact with mafic silicate grains surrounding the assemblages) tend to have minor-element compositions similar to those of unmelted chromite grains distant from the assemblages. The same relationship holds for chromite within veinlets; these grains are in contact with surrounding silicate and tend to have the same composition as unmelted chromite grains. Angular unmelted chromite grain fragments in some assemblages (e.g., Hualapai Wash assemblages A' and C) are virtually identical in composition to unmelted chromite grains in the matrix (e.g., Hualapai Wash grain C') (Table 3).

In MIL 99301, chromite grains in a large chromite-plagioclase assemblage average 11.6 wt.% Al_2O_3 (Rubin, 2002b); the coarsest grain in this particular assemblage (a grain that is completely surrounded by plagioclase) contains 17.4 wt.% Al_2O_3. Chromite grains in other assemblages in MIL 99301 that are in contact with mafic silicate grains surrounding the assemblages have much lower Al_2O_3, i.e., 5.7 wt.%, the same as in unmelted chromite grains in the matrix (Table 3).

Chromite phenocrysts within chromite-rich chondrules vary in composition; their compositions span and extend beyond the range of chromite in chromite-plagioclase assemblages. The mean composition of chromite in individual chromite-rich chondrules is relatively rich in Al_2O_3 (e.g., 21.8 wt.% in Mg1a from Magombedze; Table 3). In addition to chromite, a few chromite-rich chondrules contain ilmenite with appreciable concentrations of MgO (4–5 wt.%; A.N. Krot, unpublished data, 1993).

Plagioclase compositions are listed in Table 4. In most chromite-plagioclase assemblages, the plagioclase end-member compositions are sodic; i.e., $Ab_{80-85}Or_{2.7-6.6}$. These values are similar to the mean values in equilibrated OC: $Ab_{81.9}Or_{5.8}$, $Ab_{84.2}Or_{5.6}$, and $Ab_{85.9}Or_{3.6}$ in H, L and LL chondrites, respectively (Van Schmus and Ribbe, 1968).

There are some chromite-plagioclase assemblages that have much higher CaO/Na_2O ratios: Hualapai Wash A and C have plagioclase end-member compositions of $Ab_{65.4}Or_{3.3}$ and $Ab_{51.8}Or_{3.2}$, respectively. These more calcic plagioclase values are similar to mesostasis compositions in some chromite-rich chondrules (e.g., $Ab_{61.5}Or_{1.5}$ in Mg1a in Magombedze). Other chromite-rich chondrules have sodic mesostases (e.g., $Ab_{81.3}Or_{6.3}$ in Estacado D), similar to plagioclase in the majority of chromite-plagioclase assemblages.

Although plagioclase composition in the assemblages does not correlate with chromite grain size, it does appear to correlate with the plagioclase/chromite modal abundance ratio (Table 4). Both assemblages with calcic plagioclase compositions (Hualapai Wash A and C) have lower plagioclase/chromite modal abundance ratios (0.3 and 0.8, respectively) than the assemblages with sodic plagioclase (1 - 20).

Plagioclase in the assemblages contains 0.31 ± 0.23 wt.% Cr_2O_3 (range: 0.06–0.89 wt.%). A related inclusion in L6 Los Martinez contains plagioclase with comparable amounts of Cr_2O_3 (0.46 ± 0.51 wt.%; Brearley et al., 1991). It is possible that the Cr_2O_3 enrichments in the plagioclase analyses are an artifact caused by fluorescence of Cr from nearby chromite grains. Additional analytical work is required to determine if this is the case. However, if the Cr_2O_3 enrichments are real, they may be due to the Cr^{3+} cation substituting for Al^{3+} in the plagioclase structure where it is distributed among the tetrahedral sites. The apparent Cr_2O_3 contents of plagioclase in the assemblages are much higher than those of coarse crystalline plagioclase in equilibrated OC: <0.02 wt.% in Guareña, H6 (Allen and Mason, 1973); <0.02 wt.% in Modoc (1905), L6 (Allen and Mason, 1973); and <0.04 wt.% in the matrix of MIL 99301, LL6 (Rubin, 2002b). These Cr_2O_3 concentrations are below the detection limits of electron microprobes under normal operating conditions.

4. DISCUSSION

4.1. Formation of chromite varieties affected by shock metamorphism

4.1.1. Chromite transected by opaque shock veins

Silicate darkening in OC is caused by the dispersion of tiny grains of metallic Fe-Ni and/or troilite within silicate grain interiors and at silicate grain boundaries. In many cases, the opaque grains occur in curvilinear trails that fill fractures within the silicate grains (Rubin, 1992). This phenomenon, also referred to as "shock darkening" (e.g., Dodd, 1981) and "shock blackening" (e.g., Stöffler et al., 1991), arises from shock heating of localized areas of an OC above the Fe-FeS eutectic temperature of 988°C. Metal and troilite are melted in roughly eutectic weight-ratio proportions of 1:7.5 (Brandes and Brook, 1992) and mobilized.

Troilite grains unconnected to metal have a much higher melting temperature (i.e., ~1160°C; Brandes and Brook, 1992), above the OC solidus temperature (~1100°C; Jurewicz et al., 1995), but appreciably lower than those of olivine grains in which metal-free, troilite curvilinear trails occur (1560–1700°C for Fa_{17-32} olivines, characteristic of OC). It is thus possible that the troilite trails could have formed by impact melting of pure troilite without the surrounding olivine grains being melted as well. However, it is possible that some of the troilite trails resulted from phase separation of troilite from a metal-troilite melt during mobilization and transport. In some cases this may have involved evaporation and dissociation of troilite, vapor transport of S_2 molecules, condensation within fractures and combination with metallic Fe to form troilite (Rubin, 2002a).

The FeS and Fe-FeS melting temperatures are both far below those of pure chromite. This phase begins to melt (incongruently under equilibrium conditions) only at ~1635°C; Fig. 2129 of Levin et al., 1969). Unmelted chromite grains

Table 4. Composition of plagioclase (wt.%) in chromite-plagioclase assemblages and chromite-rich chondrules in ordinary chondrites.

variety	4	4	4	4	4	4
meteorite	Farmington	Jartai	Hualapai Wash	Hualapai Wash	Hualapai Wash	MIL 99301
grn/asmb	B	E	A	A′	C	1
# points	4	4	4	3	2	5
SiO_2	65.3	65.5	60.2	65.0	57.0	65.1
TiO_2	0.11	<0.04	0.04	0.06	0.09	0.07
Al_2O_3	20.7	21.3	25.2	21.9	27.3	21.8
Cr_2O_3	0.35	0.06	0.41	0.24	0.21	0.28
FeO	0.49	0.53	0.40	0.54	0.58	0.59
MgO	0.17	<0.04	<0.04	<0.04	<0.04	<0.04
CaO	2.4	2.6	6.5	2.4	8.8	2.7
Na_2O	9.9	10.0	7.5	9.1	5.6	8.3
K_2O	1.0	0.49	0.58	1.1	0.53	0.87
total	100.4	100.5	100.8	100.3	100.1	99.7
mol% Ab	83.3	85.0	65.4	81.6	51.8	80.1
mol% Or	5.5	2.7	3.3	6.5	3.2	5.5
plag/crm	2	7	0.3	2	0.8	2

variety	4	4	4	4	6	6
meteorite	Kernouvé	Kernouvé	Guareña	Estacado	Estacado	Magombedze[§]
grn/asmb	A	A′	A	B	D	Mg1a
# points	1	3	4	2	2	2
SiO_2	64.3	65.2	65.9	65.9	64.8	57.4
TiO_2	0.11	0.08	0.07	0.05	<0.04	0.33
Al_2O_3	21.5	21.3	21.4	21.6	21.2	25.4
Cr_2O_3	0.89	0.21	0.33	0.11	0.20	0.18
FeO	0.66	0.33	0.26	0.49	0.60	0.33
MgO	0.05	<0.04	<0.04	<0.04	<0.04	<0.04
CaO	2.7	2.5	2.6	2.5	2.6	7.6
Na_2O	9.4	9.7	9.9	9.7	9.4	7.0
K_2O	1.0	1.2	0.99	1.1	1.1	0.26
total	100.6	100.5	101.4	101.4	99.9	98.5
mol% Ab	81.4	81.7	82.6	82.2	81.3	61.6
mol% Or	5.7	6.6	5.4	6.1	6.3	1.5
plag/crm	6	4	1	20		

Petrographic varieties of chromite listed in Table 2.
grn/asmb = grain or assemblage label.
plag/crm = plagioclase/chromite modal abundance ratio.
[§] Plagioclase in this chromite-rich chondrule was analyzed by A.N. Krot (unpublished data, 1993).

transected by opaque veins (e.g., Fig. 1c,d) thus must have acquired their veins at temperatures between 988 (where Fe-FeS melted) and 1635°C (where chromite would have melted). This range can be further constrained. In many type-6 OC, coarse crystalline plagioclase grains of composition An 10–12 mol.% located near the chromite grains with opaque veins are themselves unmelted; thus, the upper limit on temperature is actually ~1120°C, the binary solidus temperature for plagioclase of this composition at 10^5 Pa (1 atm) pressure.

Chromite grains transected by opaque veins form at the same time as silicate darkening develops in the whole rock. This is consistent with the observation that many chromite grains containing troilite veins in shocked chondrites are adjacent to silicate grains that also have troilite veins transecting them (Fig. 1c,d).

4.1.2. Chromite-plagioclase assemblages

During a collision, each hypervelocity shock wave passes a given point in the target rock in less than a second. Successive hypervelocity waves (including reflected waves) can lead to significant heating caused by highly localized stress concentrations (Rinehart, 1968). Experimental studies of shock-loaded basalt indicate that the most compressible phase is plagioclase (Schaal et al., 1979). Plagioclase has a low impedance to shock compression, indicating that a greater proportion of shock wave energy is converted into heating the crystal lattice than is the case for many other silicate phases. Thus, localized shock-heating would be expected to produce plagioclase-rich impact-melt products. This is indeed the case; melt-pocket glasses in OC have plagioclase-rich compositions (Dodd and Jarosewich, 1979, 1982). These melt pockets formed by preferential in situ melting of plagioclase and lesser degrees of melting of associated components.

Small chromite grains occur in many melt pockets (Dodd and Jarosewich, 1982) suggesting that the hot plagioclase melt may have melted adjacent chromite grains. This suggestion is supported by the observation that the same shocked chondrites that possess chromite-plagioclase assemblages generally also

contain unmelted chromite grains that are not adjacent to plagioclase. Metal-troilite assemblages also have a low (eutectic) melting point (988°C) and could also be melted by a hot plagioclase melt. This is consistent with the observations of Dodd and Jarosewich (1982) who reported that metal and sulfide occur in every melt pocket that they studied.

It does not seem likely that the large impedance mismatch between plagioclase and chromite caused substantial shock reverberations at the grain boundaries between these phases in most S3-S5 OC so that relatively large fractions of chromite melted. The impedance mismatch between metallic Fe-Ni and mafic silicate grains is also high and there is no evidence of widespread melting at metal-silicate grain boundaries in S3-S5 OC. If the shock pressures were high, differences in shock impedance could lead to high-pressure phase transformations at grain boundaries where shock-wave reverberations tend to prolong the high-pressure regime (A. El Goresy, pers. commun., 2002). If such conditions prevailed in the chromite-plagioclase assemblages, plagioclase might be expected to have been transformed into the high-pressure polymorph with the hollandite structure (Liu, 1978). This phase was identified as intergrowths with feldspathic glass in patches that petrographically resemble maskelynite in the L6, S5 chondrite Sixiangkou (Gillet et al., 2000). Patches that appear to be maskelynite are not typically associated with chromite-plagioclase assemblages in S3-S5 OC. It thus seems probable that typical chromite-plagioclase assemblages do not contain plagioclase with the hollandite structure and were thus not formed mainly by shock-wave reverberations caused by the impedance mismatch between plagioclase and chromite.

Chromite-plagioclase melts produced by impacts are relatively rich in bulk Al_2O_3. In many cases, chromite grains crystallizing from these melts are richer in Al_2O_3 than typical unshocked chromite grains that grew in type-4–6 OC during thermal metamorphism. The chromite grains in the assemblages that crystallized before plagioclase will be richer in Al_2O_3 than those chromite grains that crystallized after the onset of plagioclase crystallization (e.g., El Goresy et al., 1976). Rare TiO_2-rich chromite grains in chromite-plagioclase assemblages probably formed from melts that were enriched in Ti because their precursor chromite grains contained ilmenite or rutile.

Chromite grains in the PAT 91501 l-chondrite impact-melt rock (Mittlefehldt and Lindstrom, 2001) tend to be richer in Al_2O_3 (up to 9.2 wt.%) or TiO_2 (up to 7.6 wt.%) than those in typical equilibrated L chondrites (3.7–6.3 wt.% Al_2O_3; 1.5–3.4 wt.% TiO_2; Bunch et al., 1967).

The chromite-plagioclase melts are also relatively rich in bulk Cr_2O_3. Not all of the Cr_2O_3 partitions into chromite during rapid cooling. Some is incorporated into the plagioclase or remains in the residual melt that transforms into plagioclase-rich glass during quenching. This scenario could account for the relatively high Cr_2O_3 contents of plagioclase in the chromite-plagioclase assemblages (Table 4), assuming that these concentrations are not analytical artifacts caused by fluorescence.

The two chromite-plagioclase assemblages with relatively calcic plagioclase and low plagioclase/chromite modal abundance ratios (Table 4) may have formed at higher shock temperatures. The most probable mechanism for creating high Ca contents is the evaporation of a large fraction (>50%) of the alkalies; this could also lead to a diminishment in the proportion of plagioclase in the melt.

Because of similarities in shape and size, it seems likely that most chromite grains in individual chromite-plagioclase assemblages share the same history. If it is likely that an Al_2O_3-rich chromite in a particular assemblage crystallized from a melt, then the other chromite grains probably did so as well. The fact that chromite grains at the surfaces of the chromite-plagioclase assemblages, adjacent to mafic silicate grains, tend to have approximately the same minor-element compositions as unmelted chromite grains in the host probably reflects equilibration during annealing (as documented by Bunch et al., 1967). Chromite grains in the assemblages completely surrounded by plagioclase or plagioclase glass tend to be richer in Al_2O_3 because the surrounding glass retarded diffusive exchange with chromite grains in the matrix.

Some assemblages appear to contain relict, unmelted chromite grains (e.g., Fig. 2c). In such cases, it seems likely that the plagioclase melt was not hot enough to melt adjacent chromite. The relict, angular chromite grain fragments in these assemblages retained their minor-element concentrations.

These models for the production of chromite-plagioclase assemblages need to be tested experimentally. Chromite Hugoniot data are required. Experiments of the impact-melting behavior of chromite and chromite-plagioclase associations should be conducted.

4.1.3. Chromite veinlets

The occurrence in many shocked chondrites of chromite veinlets that transect mafic silicate grains in the vicinity of chromite-plagioclase assemblages suggests a petrogenetic relationship between the veinlets and the assemblages.

As stated above, it is not possible for the chromite veinlets to have formed by the melting of pure chromite because the (incongruent) equilibrium melting temperature of chromite is ~1635°C. If the chromite had been heated to this temperature (far above that of the OC solidus), the surrounding silicates would also have melted (particularly in L and LL chondrites), contrary to observation.

The occurrence of plagioclase glass in some chromite veinlets (particularly in Jartai; Fig. 1f) suggests that the veinlets formed in a manner analogous to the formation of chromite-plagioclase assemblages. I suggest the following scenario: chromite-plagioclase melts were injected into preexisting fractures in adjacent silicate grains; as the temperature fell and the discharge of melts through the fractures decreased, chromite crystallized in the fractures and the plagioclase-rich melts flowed onward to form nearby plagioclase-glass-rich, chromite-poor melt pockets. The close proximity of some veinlets and melt pockets is illustrated in Figure 1f. In most veinlets, the plagioclase melt completely withdrew; in a few cases (e.g., Fig. 1f), patches of melt remained.

4.1.4. Relationship of chromite-plagioclase assemblages to chromite-rich chondrules

There are two possibilities for the formation locations of chromite-rich chondrules: the solar nebula and asteroidal parent

bodies. Although a nebular origin for normal mafic silicate chondrules is widely accepted (e.g., McSween, 1977; Clayton et al., 1983; Taylor et al., 1983; Grossman, 1988; Hewins, 1989, 1997; Wasson, 1993; Alexander, 1994; Boss, 1996; Scott et al., 1996; Connolly and Love, 1998; Rubin, 2000; Krot et al., 2001; Desch and Connolly, 2002), chromite-rich chondrules do not occur in primitive type-3 chondrites, mitigating against a nebular origin.

Coarse grains of chromite are absent from primitive type-3 chondrites (Huss et al., 1981); they nucleate and grow in OC during annealing. The presence of chromite-rich chondrules in type-4–6 OC (and their absence in primitive type-3 OC) suggests that these chondrules formed from chromite-rich precursors within asteroids. The presence of these chondrules in shocked type-4–6 OC (e.g., Elenovka, S3; Richmond, S4; Rose City, S6) and in OC regolith breccias (e.g., Dimmitt; Ipiranga; Menow; Pantar; Plainview; Tysnes Island; Weston; A. N. Krot, unpublished data, 1993) is consistent with a parent-body shock origin.

Although chromite-plagioclase assemblages are generally devoid of mafic silicates, many chromite-rich chondrules contain olivine (Fig. 3a,b) and some contain pyroxene. Nevertheless, it seems plausible that these chondrules formed in a manner analogous to that of chromite-plagioclase assemblages, i.e., by impact melting chromite, plagioclase and adjacent mafic silicates. The presence of silicate indicates that higher shock energies are required to form the chromite-rich chondrules than the silicate-free chromite-plagioclase assemblages. In this model, the melt must have been jetted from the impact site and then formed droplets due to surface tension. If this is correct, the chromite-rich chondrules are not nebular products; they formed in a manner analogous to chondrule-like crystalline spherules from the Moon (e.g., King et al., 1972), achondrites (Brownlee and Rajan, 1973) and terrestrial impact craters (Graup, 1981).

Crystallization of the chromite-rich chondrules probably commenced while the droplets were in flight before landing on the parent-body surface. Because of the high plagioclase content of the precursors, the bulk melts have high Al_2O_3 contents. Chromite grains crystallizing from these melts tend to be appreciably richer in Al_2O_3 than unmelted chromite grains in the same meteorites. (The same process accounts for the relatively high Al_2O_3 contents of chromite grains surrounded by plagioclase in chromite-plagioclase assemblages.)

4.2. Use of chromite-plagioclase assemblages as a shock indicator

The occurrence of chromite-plagioclase assemblages in shock-stage S6 impact melt breccias, shock-stage S3-S5 rocks, and OC regolith breccias strongly supports the hypothesis that these assemblages were formed by shock processes. Although chromite-plagioclase assemblages also occur in S1 rocks of petrologic type-5 and −6, these particular rocks possess additional shock indicators (e.g., silicate darkening, abundant occurrences of metallic Cu, polycrystalline troilite, opaque veins) that demonstrate that the rocks were shocked and later annealed (see below).

Most of the S2 rocks that contain chromite-plagioclase assemblages and chromite veinlets also possess additional shock indicators. LL6 Elbert exhibits silicate darkening and contains metal-sulfide veinlets and narrow glassy pseudotachylite-like veins. H5 NWA 141 exhibits silicate darkening and contains rapidly solidified metal-troilite intergrowths, irregular troilite grains within metallic Fe-Ni, and metallic Cu. H6 Ogi exhibits silicate darkening and contains metallic Cu, irregular grains of troilite within metal, rapidly solidified metal-troilite intergrowths, opaque veins, and plagioclase-rich melt pockets. H6 Queen's Mercy exhibits moderate silicate darkening and contains irregular grains of troilite within metal, metal and sulfide veins, and irregular patches of apparently mobilized plagioclase; Turner et al. (1978) reported thin, black pseudotachylite-like shock veins in Queen's Mercy. H5 Richardton contains polycrystalline troilite and metallic Cu. LL5 Alta'ameem contains metallic Cu and irregular grains of troilite within metallic Fe-Ni. H6 Xingyang exhibits silicate darkening and contains rare metallic Fe-Ni grains with included irregular masses of troilite. These S2 OC were probably shocked initially to ≥S3 levels and then annealed.

Because it seems unlikely that a shocked OC could be annealed so precisely that its olivine would heal planar fractures and planar deformation features, lose mosaic extinction, but retain undulose extinction (characteristic of shock-stage S2), it is more probable that an OC would be annealed to S1 levels so that its olivine would develop sharp optical extinction. I surmise that these OC were shocked again, after annealing, to shock-stage S2 levels.

It thus seems that chromite-plagioclase assemblages in OC occur exclusively in shocked rocks or those that have been shocked and annealed. The identification of chromite-plagioclase assemblages and chromite veinlets in an OC constitutes sufficient evidence in and of itself to conclude that the rock was once shocked to at least shock-stage S3. Other shock indicators expected in an S3 OC in the absence of annealing include opaque shock veins, melt pockets, undulose extinction in various silicate phases, and planar fractures in olivine (Stöffler et al., 1991).

Chromite-plagioclase assemblages probably begin to form in OC at equilibrium shock pressures below those necessary to cause mosaic extinction in olivine (i.e., <10–15 GPa). The assemblages also form at higher shock stages including those that correspond to S6 impact-melt breccias (which experienced equilibrium shock pressures ≥45–60 GPa).

4.3. Implications for shock and thermal history of shock-stage S1 ordinary chondrites

Although the olivine grains in MIL 99301 exhibit sharp optical extinction characteristic of a shock-stage S1 (i.e., unshocked) chondrite, many petrographic features of the rock indicate that it once experienced intense shock metamorphism to levels corresponding to shock-stage ~S4 (Rubin, 2002b). These features include: (1) extensive silicate darkening caused by the dispersion within and around silicate grains of curvilinear trails of metallic Fe-Ni and troilite (Rubin, 1992); (2) polycrystalline troilite, shown by shock-recovery experiments to form at shock pressures of 35 to 60 GPa (Schmitt et al., 1993); (3) myrmekitic plessite, formed by the localized shock melting of abutting kamacite and taenite grains (Rubin, 2002b); (4) a relatively high occurrence abundance of metallic Cu,

reflecting the localized shock-melting of metal-troilite assemblages, crystallization of taenite, supersaturation of Cu in the residual sulfide-rich melt, and nucleation of small patches of metallic Cu at high-surface-energy sites (Rubin, 1994); (5) coarse grains of low-Ca clinopyroxene with polysynthetic twinning, which form from orthopyroxene at pressures exceeding ~5 GPa (Hornemann and Müller, 1971; Stöffler et al., 1991); and (6) chromite-plagioclase assemblages, which are abundant in MIL 99301 (Rubin, 2002b).

The occurrence of chromite-plagioclase assemblages and chromite veinlets along with other shock indicators (e.g., silicate darkening, metallic Cu, opaque veins, polycrystalline troilite) in every type-5 and −6 OC of shock-stage S1 that I examined (i.e., 25 out of 25) indicates that these highly metamorphosed rocks were significantly shocked and then annealed. The only viable heat source capable of causing postmetamorphic annealing is an impact. Annealing probably was caused by residual impact heat associated with the collision that caused the shock effects. The shocked and annealed rock could have been deposited within a hot ejecta blanket or beneath the crater floor in proximity to lenses of impact melts. In the case of MIL 99301, ^{39}Ar-^{40}Ar analysis indicates that the rock experienced a major degassing event ~4.26 Ga ago, consistent with substantial heating (Dixon et al., 2003). At this late date, i.e., ~300 Ma after accretion, an impact event is the only plausible heat source.

It is likely that other shock-stage S1 OC of petrologic type 5 or 6 were also annealed by residual impact heat associated with the collisions that shocked these rocks initially. ^{39}Ar-^{40}Ar age-dating indicates that, in many cases, these shock events occurred very early in the history of the parent asteroids. The Ar-Ar plateau ages of the S1, H6 chondrites Guareña, Kernouvé and Portales Valley are 4.44±0.03, 4.45±0.03 and 4.477±0.016 Ga, respectively (Turner et al., 1978; Garrison and Bogard, 2001). The near-simultaneity of metamorphism and shock in these particular OC within ~100 Ma of accretion is consistent with impact heating being a major mechanism responsible for metamorphosing ordinary chondrites (Wasson et al., 1987; Cameron et al., 1990; Rubin, 1995b).

Although the majority of equilibrated OC may be fragmental breccias containing a few compositionally aberrant silicate and metal grains (Scott et al., 1985; Rubin, 1990), brecciation cannot be responsible for S1 or S2 OC exhibiting petrographic shock indicators common to rocks of higher shock stages. In these S1 and S2 OC, those olivine grains that happen to be adjacent to the shock indicators (e.g., chromite veinlets, chromite-plagioclase assemblages, polycrystalline troilite, martensite) exhibit the same low-shock optical properties (i.e., sharp or slightly undulose extinction, no planar fractures) as the other olivine grains in the same thin sections.

5. CONCLUSIONS

Chromite-plagioclase assemblages are a reliable shock indicator in ordinary chondrites, indicating shock levels of at least shock-stage S3. The assemblages are common in shock-stage-S6 impact-melt breccias and occur in nearly every shock-stage S3-S5 OC. Plagioclase has a low impedance to shock compression, i.e., shock caused plagioclase to melt. Hot plagioclase melts may have melted adjacent chromite and formed chromite-plagioclase assemblages. Those chromite grains that are completely surrounded by plagioclase in the assemblages are generally richer in Al_2O_3 than unmelted, matrix chromite grains (that are not adjacent to plagioclase) in the same meteorite.

Chromite veinlets commonly occur in the vicinity of chromite-plagioclase assemblages and formed in an analogous manner. A chromite- and plagioclase-rich melt was injected into surrounding fractures in silicate grains, chromite crystallized within the fracture and the plagioclase-rich melt flowed onward and pooled to form nearby plagioclase-rich melt pockets.

Chromite-rich chondrules probably formed during higher-energy shock events by impact melting of chromite, plagioclase and adjacent silicate. The melt was jetted from the impact site and formed droplets due to surface tension. Crystallization probably commenced in flight, before landing on the asteroid surface.

The occurrence of chromite-plagioclase assemblages in highly metamorphosed, shock-stage S1 OC suggests that these rocks were once shocked to levels of at least shock-stage S3 and then annealed by residual heat generated by the shock itself. The rocks may have been buried in proximity to impact melts beneath the crater floor or near hot debris in an ejecta blanket. Ar-Ar age data indicate that, in many cases, these events occurred very early in the history of their parent asteroids. Shock-stage S2 OC containing chromite-plagioclase assemblages may have experienced an identical history except for being shocked again after annealing. It seems possible that some equilibrated OC of shock stages S3-S6 were also shocked, annealed and shocked again.

Acknowledgments—I thank J. T. Wasson for comments, D. D. Bogard for discussions, and F. T. Kyte for technical assistance. I am grateful to A. N. Krot for permission to use his unpublished data on chromite-rich chondrules. I also thank the Smithsonian Institution, the Institute of Meteoritics at the University of New Mexico, the Institute of Planetology at the University of Münster, and the Antarctic Meteorite Working Group for the loan of thin sections. The manuscript benefited from helpful reviews by G. R. Huss and R. T. Schmitt. This work was supported in part by NASA Grant No. NAG5–4766 (A. E. Rubin).

Associate editor: Christian Koeberl

REFERENCES

Alexander C. M. O. (1994) Trace element distributions within ordinary chondrite chondrules: Implications for chondrule formation conditions and precursors. *Geochim. Cosmochim. Acta.* **58,** 3451–3467.

Allen R. O. and Mason B. (1973) Minor and trace elements in some meteoritic minerals. *Geochim. Cosmochim. Acta.* **37,** 1435–1456.

Anders E. (1964) Origin, age, and composition of meteorites. *Space Sci. Rev.* **3,** 583–714.

Ashworth J. R. (1985) Transmission electron microscopy of L-group chondrites, 1. Natural shock effects. *Earth Planet. Sci. Lett.* **73,** 17–32.

Begemann F. and Wlotzka F. (1969) Shock induced thermal metamorphism and mechanical deformations in Ramsdorf chondrite. *Geochim. Cosmochim. Acta.* **33,** 1351–1370.

Bennett M. E. and McSween H. Y. (1996) Shock features in iron-nickel metal and troilite of L-group ordinary chondrites. *Earth Planet. Sci. Lett.* **31,** 255–264.

Binns R. A., Davis R. J., and Reed S. J. B. (1969) Ringwoodite, a natural $(Mg,Fe)_2SiO_4$ spinel in the Tenham meteorite. *Nature.* **221,** 943–944.

Bischoff A. and Keil K. (1984) Al-rich objects in ordinary chondrites: Related origin of carbonaceous and ordinary chondrites and their constituents. *Geochim. Cosmochim. Acta.* **48,** 693–709.

Bogard D. D. (1979) Chronology of asteroid collisions as recorded in meteorites. In *Asteroids* (ed. T. Gehrels and M. S. Matthews), pp. 558–578. University of Arizona Press.

Bogard D. D., Garrison D. H., Norman M., Scott E. R. D., and Keil K. (1995) ^{39}Ar-^{40}Ar age and petrology of Chico: large-scale impact melting on the L-chondrite parent body. *Geochim. Cosmochim. Acta.* **59,** 1383–1400.

Boss A. P. (1996) A concise guide to chondrule formation models. In *Chondrules and the Protoplanetary Disk* (ed. R. H. Hewins, R. H. Jones, and E. R. D. Scott), pp. 257–263. Cambridge Univ.

Brandes E. A. and Brook G. B. (1992) *Smithells Metal Reference Handbook*., 7th Ed:, Butterworth-Heinemann. ca.1600 pp.

Brearley A. J., Casanova I., Miller M. L., and Keil K. (1991) Mineralogy and possible origin of an unusual Cr-rich inclusion in the Los Martinez (L6) chondrite. *Meteoritics.* **26,** 287–301.

Brownlee D. E. and Rajan R. S. (1973) Micrometeorite craters discovered on chondrule-like objects from Kapoeta meteorite. *Science.* **182,** 1341–1344.

Bunch T. E., Keil K., and Snetsinger K. G. (1967) Chromite composition in relation to chemistry and texture of ordinary chondrites. *Geochim. Cosmochim. Acta.* **31,** 1569–1582.

Buseck P. R. and Keil K. (1966) Meteoritic rutile. *Am. Mineral.* **51,** 1506–1515.

Cameron A. G. W., Benz W., and Wasson J. T. (1990) Heating during asteroidal collisions (abstract). *Lunar Planet. Sci.* **21,** 155–156.

Clayton R. N., Onuma N., Ikeda Y., Mayeda T., Hutcheon I. D., Olsen E. J. and Molini-Velsko C. (1983) Oxygen isotopic compositions of chondrules in Allende and ordinary chondrites. In *Chondrules and their Origins* (ed. E. A. King), pp. 37–43. Lunar Planet. Inst.

Coleman L. C. (1977) Ringwoodite and majorite in the Catherwood meteorite. *Can. Mineral.* **15,** 97–101.

Connolly H. C. and Love S. G. (1998) The formation of chondrules: Petrologic tests of the shock wave model. *Science.* **280,** 62–67.

Desch S. J. and Connolly H. C. (2002) A model of the thermal processing of particles in solar nebula shocks: Application to the cooling rates of chondrules. *Meteorit. Planet. Sci.* **37,** 183–207.

Dixon E. T., Bogard D. D. and Rubin A. E. (2003) ^{39}Ar-^{40}. Ar evidence for an ~4.26 Ga impact heating event on the LL parent body. *Lunar Planet. Sci.* **34**, abstract#1108, Lunar and Planetary Institute, Houston.

Dodd R. T. (1981) Meteorites—A Petrologic-Chemical Synthesis, *Cambridge*. 368 pp.

Dodd R. T. and Jarosewich E. (1979) Incipient melting and shock classification of L-group chondrites. *Earth Planet. Sci. Lett.* **44,** 335–340.

Dodd R. T. and Jarosewich E. (1982) The compositions of incipient shock melts in L6 chondrites. *Earth Planet. Sci. Lett.* **59,** 355–363.

El Goresy A., Prinz M. and Ramdohr P. (1976) Zoning in spinels as an indicator of the crystallization histories of mare basalts. *Proc. Lunar Sci.Conf.* **7th**, 1261–1279.

Fodor R. V. and Keil K. (1976) Carbonaceous and noncarbonaceous lithic fragments in the Plainview, Texas chondrite: origin and history. *Geochim. Cosmochim. Acta.* **40,** 177–189.

Garrison D. H. and Bogard D. D. (2001) ^{39}Ar-^{40}Ar and space exposure ages of the unique Portales Valley H-chondrite. *Lunar Planet. Sci.* **32**, abstract#1137, Lunar and Planetary Institute, Houston.

Gillet P., Chen M., Dubrovinsky L., and El Goresy A. (2000) Natural $NaAlSi_3O_8$-hollandite in the shocked Sixiangkou meteorite. *Science* **287,** 1633–1636.

Grady M. M. (2000) *Catalogue of Meteorites,* 5th Ed., Cambridge Univ. Press. 689 pp.

Graup G. (1981) Terrestrial chondrules, glass spherules and accretionary lapilli from the suevite, Ries Crater, Germany. *Earth Planet. Sci. Lett.* **55,** 407–418.

Grossman J. N. (1988) Formation of chondrules. In *Meteorites and the Early Solar System* (ed. J. F. Kerridge and M. S. Matthews), pp. 680–696. Univ. Arizona Press.

Hewins R. H. (1989) The evolution of chondrules. *Proc. NIPR Symp. Antarct. Met.* **2,** 200–220.

Hewins R. H. (1997) Chondrules. *Ann. Review of Earth and Planetary Science.* **25,** 61–83.

Heymann D. (1967) On the origin of hypersthene chondrites: Ages and shock effects of black chondrites. *Icarus.* **6,** 189–221.

Hornemann U. and Müller W. F. (1971) Shock-induced deformation twins in clinopyroxene. *Neues Jahrb. Mineral.* **6,** 247–256.

Huss G. R., Keil K., and Taylor G. J. (1981) The matrices of unequilibrated ordinary chondrites: Implications for the origin and history of chondrites. *Geochim. Cosmochim. Acta.* **45,** 33–51.

Hutson M. (1989) Shock effects in H-group chondrites (abstract). *Lunar Planet. Sci.* **20,** 436–437.

Jurewicz A. J. G., Mittlefehldt D. W., and Jones J. H. (1995) Experimental partial melting of the St. Severin (LL) and Lost City (H) chondrites. *Geochim. Cosmochim. Acta.* **59,** 391–408.

Keil K., Kirchner E., Gomes C. B., and Nelen J. (1977) Studies of Brazilian meteorites V. Evidence for shock metamorphism in the Paranaiba, Mato Grosso, chondrite. *Rev. Brasil. Geosci.* **7,** 256–268.

King E. A., Carman M. F., and Butler J. C. (1972) Chondrules in Apollo 14 samples: Implications for the origin of chondritic meteorites. *Science.* **175,** 59–60.

Kring D. A., Swindle T. D., Britt D. T., and Grier J. A. (1996) Cat Mountain: A meteoritic sample of an impact-melted asteroid regolith. *J. Geophys. Res.* **101,** 29353–29371.

Kring D. A., Hill D. H., Gleason J. D., Britt D. T., Consolmagno G. J., Farmer M., Wilson S., and Haag R. (1999) Portales Valley: A meteoritic sample of the brecciated and metal-veined floor of an impact crater on an H-chondrite asteroid. *Meteorit. Planet. Sci.* **34,** 663–669.

Krot A. N., Meibom A., Russell S. S., Alexander C.M.O'D., Jeffries T. E., and Keil K. (2001) A new astrophysical setting for chondrule formation. *Science.* **291,** 1776–1779.

Krot A. N. and Rubin A. E. (1993) Chromite-rich mafic silicate chondrules in ordinary chondrites: Formation by impact melting (abstract). *Lunar Planet. Sci.* **24,** 827–828.

Krot A. N., Zolensky M. E., Wasson J. T., Scott E. R. D., Keil K., and Ohsumi K. (1997) Carbide-magnetite assemblages in type-3 ordinary chondrites. *Geochim. Cosmochim. Acta.* **61,** 219–237.

Levin E. M., Robbins C. R. and McMurdie H. F. (1969) *Phase Diagrams for Ceramists: 1969 Supplement,* American Ceramic Society. 625 pp.

Liu L.-G. (1978) High-pressure phase transformations of albite, jadeite and nepheline. *Earth Planet. Sci. Lett.* **37,** 438–444.

Mason B. and Wiik H. B. (1966) The composition of the Bath, Frankfort, Kakangari, Rose City, and Tadjera meteorites. *Am. Mus. Nov.* **2272,** 1–24.

McSween H. Y. (1977) Chemical and petrographic constraints on the origin of chondrules and inclusions in carbonaceous chondrites. *Geochim. Cosmochim. Acta.* **41,** 1843–1860.

Mittlefehldt D. W. and Lindstrom M. M. (2001) Petrology and geochemistry study of Patuxent Range 91501, a clast-poor impact melt from the L-chondrite parent body and Lewis Cliff 88663, an L7 chondrite. *Meteorit. Planet. Sci.* **36,** 439–457.

Noonan A. F. and Nelen J. A. (1976) A petrographic and mineral chemistry study of the Weston, Connecticut, chondrite. *Meteoritics.* **11,** 111–131.

Pellas P. and Fiéni C. (1988) Thermal histories of ordinary chondrite parent asteroids (abstract). *Lunar Planet. Sci.* **19,** 915–916.

Pellas P. and Storzer D. (1981) ^{244}Pu fission track thermometry and its application to stony meteorites. *Proc. R. Soc. Lond. A.* **374,** 253–270.

Pellas P., Fiéni C., Trieloff M., and Jessberger E. K. (1990) Metamorphism intervals of equilibrated H and L chondrites as defined by ^{244}Pu chronometry and Ar-Ar ages (abstract). *Meteoritics.* **25,** 397.

Ramdohr P. (1967) Chromite and chromite chondrules in meteorites - I. *Geochim. Cosmochim. Acta.* **31,** 1961–1967.

Ramdohr P. (1973) *The Opaque Minerals in Stony Meteorites*, Elsevier. 245 pp.

Rinehart J. S. (1968) Intense destructive stresses resulting from stress wave interactions. In *Shock Metamorphism of Natural Materials* (ed. B. M. French and N. M. Short), pp. 31–42. Mono.

Rubin A. E. (1985) Impact melt products of chondritic material. *Rev. Geophys.* **23,** 277–300.

Rubin A. E. (1990) Kamacite and olivine in ordinary chondrites: Intergroup and intragroup relationships. *Geochim. Cosmochim. Acta.* **54,** 1217–1232.

Rubin A. E. (1992) A shock-metamorphic model for silicate darkening and compositionally variable plagioclase in CK and ordinary chondrites. *Geochim. Cosmochim. Acta.* **56,** 1705–1714.

Rubin A. E. (1994) Metallic copper in ordinary chondrites. *Meteoritics.* **29,** 93–98.

Rubin A. E. (1995a) Fractionation of refractory siderophile elements in metal from the Rose City meteorite. *Meteoritics.* **30,** 415–417.

Rubin A. E. (1995b) Petrologic evidence for collisional heating of chondritic asteroids. *Icarus.* **113,** 156–167.

Rubin A. E. (2000) Petrologic, geochemical and experimental constraints on models of chondrule formation. *Earth Sci. Rev.* **50,** 3–27.

Rubin A. E. (2002a) The Smyer H-chondrite impact-melt breccia and evidence for sulfur vaporization. *Geochim. Cosmochim. Acta.* **66,** 683–695.

Rubin A. E. (2002b) Post-shock annealing of Miller Range 99301: Implications for impact heating of ordinary chondrites. *Geochim. Cosmochim. Acta.* **66,** 3327–3337.

Rubin A. E., Scott E. R. D., and Keil K. (1997) Shock metamorphism of enstatite chondrites. *Geochim. Cosmochim. Acta.* **61,** 847–858.

Rubin A. E., Ulff-Møller F., Wasson J. T., and Carlson W. D. (2001) The Portales Valley meteorite breccia: Evidence for impact-induced melting and metamorphism of an ordinary chondrite. *Geochim. Cosmochim. Acta.* **65,** 323–342.

Rubin A. E., Zolensky M. E., and Bodnar R. J. (2002) The halite-bearing Zag and Monahans. (1998) meteorite breccias: Shock metamorphism, thermal metamorphism, and aqueous alteration on the H-chondrite parent body. *Meteorit. Planet. Sci.* **37,** 125–141.

Schaal R. B., Hörz F., Thompson T. D., and Bauer J. F. (1979) Shock metamorphism of granulated lunar basalt. *Proc. Lunar Planet. Sci. Conf.* **10,** 2547–2571.

Schmitt R. T., Deutsch A., and Stöffler D. (1994) Shock recovery experiments with the H6 chondrite Kernouvé at preshock temperatures of 293 and 920 K (abstract). *Meteoritics.* **29,** 529–530.

Schmitt R. T. and Stöffler D. (1995) Classification of chondrites (abstract). *Meteoritics.* **30,** 574–575.

Scott E. R. D. (1982) Origin of rapidly solidified metal-troilite grains in chondrites and iron meteorites. *Geochim. Cosmochim. Acta.* **46,** 813–823.

Scott E. R. D., Lusby D. and Keil K. (1985) Ubiquitous brecciation after metamorphism in equilibrated ordinary chondrites. *Proc. Lunar Planet. Sci. Conf.* **16th**, D137-D148.

Scott E. R. D., Love S. G. and Krot A. N. (1996) Formation of chondrules and chondrites in the protoplanetary nebula. In *Chondrules and the Protoplanetary Disk* (ed. R. H. Hewins, R. H. Jones, and E. R. D. Scott), pp. 87–96. Cambridge University Press.

Smith B. A. and Goldstein J. I. (1977) The metallic microstructures and thermal histories of severely reheated chondrites. *Geochim. Cosmochim. Acta.* **41,** 1061–1072.

Smith J. V. and Mason B. (1970) Pyroxene-garnet transformation in Coorara meteorite. *Science.* **168,** 832–833.

Snetsinger K. G. and Keil K. (1969) Ilmenite in ordinary chondrites. *Am. Mineral.* **54,** 780–786.

Snetsinger K. G., Keil K., and Bunch T. E. (1967) Chromite from "equilibrated" *chondrites*. *Am. Mineral.* **52,** 1322–1331.

Stöffler D., Keil K., and Scott E. R. D. (1991) Shock metamorphism of ordinary chondrites. *Geochim. Cosmochim. Acta.* **55,** 3845–3867.

Taylor G. J. and Heymann D. (1969) Shock, reheating, and the gas retention ages of chondrites. *Earth Planet Sci. Lett.* **7,** 151–161.

Taylor G. J., Okada A., Scott E. R. D., Rubin A. E., Huss G. R., and Keil K. (1981) The occurrence and implications of carbide-magnetite assemblages in unequilibrated ordinary chondrites (abstract). *Lunar Planet. Sci.* **12,** 1076–1078.

Taylor G. J., Scott E. R. D., and Keil K. (1983) Cosmic setting for chondrule formation. In *Chondrules and their Origins* (ed. E. A. King), pp. 262–278. Lunar and Planetary Institute, Houston.

Turner G., Enright M. C. and Cadogan P. H. (1978) The early history of chondrite parent bodies inferred from ^{40}Ar-^{39}Ar ages. *Proc. Lunar Planet. Sci. Conf.* **9th**, 989–1025.

Wasson J. T. (1993) Constraints on chondrule origins. *Meteoritics.* **28,** 14–28.

Wasson J. T., Benz W., and Rubin A. E. (1987) Heating of primitive, asteroid-size bodies by large impacts (abstract). *Meteoritics.* **22,** 525–526.

Willis J. and Goldstein J. I. (1983) A three dimension study of metal grains in equilibrated, ordinary chondrites. *Proc. Lunar Planet. Sci. Conf.* **14th**, B287-B292.

Wood J. A. (1967) Chondrites: Their metallic minerals, thermal histories, and parent planets. *Icarus.* **6,** 1–49.